

Published in final edited form as:

Nat Med. ; 18(4): 572–579. doi:10.1038/nm.2667.

Macrophage derived Wnt signalling opposes Notch signalling in a Numb mediated manner to specify HPC fate in chronic liver disease in human and mouse

Luke Boulter^{1,2}, Olivier Govaere³, Tom G Bird^{1,2}, Sorina Radulescu⁴, Prakash Ramachandran², Antonella Pellicoro², Rachel A Ridgway⁴, Sang Soo Seo¹, Bart Spee⁵, Nico Van Rooijen^{3,6}, Owen J. Sansom⁴, John P Iredale², Sally Lowell¹, Tania Roskams³, and Stuart J Forbes^{1,2}

¹MRC Centre for Regenerative Medicine, University of Edinburgh, Edinburgh, EH16 4UU, UK

²MRC Centre for Inflammation Research, University of Edinburgh, Edinburgh, EH16 4TJ, UK

³Morphology and Molecular Pathology Section, Minderbroedersstraat 12 blok p – box 1032 3000

Leuven , Belgium ⁴The Beatson Institute for Cancer Research, Switchback Road, Glasgow G61

1BD, UK ⁵Department of Clinical Sciences of Companion Animals, Faculty of Veterinary

medicine, Utrecht University, Utrecht, The Netherlands. ⁶Vrije Universiteit VUMC, Department of

Molecular Cell Biology, Faculty of Medicine, Van der oechorststraat 71081 BT Amsterdam, The Netherlands

Abstract

During chronic injury, regeneration of the adult liver becomes impaired. In this context bipotent Hepatic Progenitor Cells (HPCs) become activated and can regenerate both cholangiocytes and hepatocytes. Notch and Wnt signalling during hepatic ontogeny are described, but their roles in HPC mediated liver regeneration are unclear. Here we show in human diseased liver and murine models of the ductular reaction with biliary and hepatocyte regeneration that Notch and Wnt signalling direct HPC specification within the activated myofibroblasts and macrophages HPC niche. During biliary regeneration, Numb is downregulated in HPCs, Jagged1 promotes biliary specification within HPCs. During hepatocyte regeneration, macrophage derived canonical Wnt signalling maintains Numb within HPCs, and Notch signalling is reduced promoting hepatocyte specification. This dominant Wnt state is stimulated through engulfment of hepatocyte debris by

Corresponding Author: Prof. Stuart Forbes, MRC Centre for Regenerative Medicine, Scottish Centre for Regenerative Medicine, 5 Little France Drive, Edinburgh, EH16 4UU. stuart.forbes@ed.ac.uk.

Author Contributions:

L.B. – Experimental design, Data generation, data analysis, manuscript preparation

O.G. – Experimental design, Data generation, data analysis

T.G.B. – Experimental design, Data generation

S.R. – Data generation

P.R. – Experimental design, Data generation

A.P. – Experimental design, Data generation

R.A.R. – Data generation

S.S.S. – Generation of 3D images

B.S. – Data generation

N.v.R. – generation and supply of clodronate liposomes

O.J.S. – Manuscript editing

J.P.I. – Experimental Design, Manuscript editing, experimental funding

S.L. – Manuscript editing, experimental design

T.R. – Manuscript editing, experimental design, experimental funding

S.J.F. – Manuscript editing, experimental design, experimental funding

niche macrophages and can directly influence the HPCs. Macrophage Wnt3a expression in turn facilitates hepatocyte regeneration – thus exemplifying a novel positive feedback mechanism in adult parenchymal regeneration.

Chronic liver disease causes high morbidity and mortality worldwide. The WHO ascribed a DALY of 37,760/100,000 people in 2004¹. The only cure for end-stage liver disease is liver transplantation, however donor organ availability cannot meet demand and many patients die. A necessary step is to understand the mechanisms controlling regeneration in chronic liver disease and identify novel pathways that could be therapeutically targeted. Moreover the liver provides a unique model of solid organ regeneration with a definite contribution from HPCs^{3, 4}. In human disease the HPCs form a critical component of the ductular reaction, which expands in an activated niche to regenerate the damaged liver^{4, 5}. Injury and regeneration are often described separately as discrete events; however the importance of the inflammatory response in cellular regeneration has been highlighted in several organs linking inflammation with both scar formation and restoration of a functional epithelium⁶⁻⁸.

During ontogeny the Notch and Wnt pathways have been implicated in the lineage specification of hepatocytes and cholangiocytes⁹⁻¹¹. The Notch signalling pathway is necessary for specification of the biliary tree, and Notch pathway ablation results in failure of hepatoblast specification into cholangiocytes^{12, 13} resulting in bile duct paucity, a characteristic of Alagilles syndrome¹³⁻¹⁶ furthermore ectopic activation of the Notch pathway in foetal hepatoblasts by over-expression of the *N^{icd}* results in hyper-arborisation of biliary ductules¹⁷. The Notch pathway comprises a family of single span receptors as well as ligand families Jagged and Delta¹⁸. Receptor–ligand interactions result in the liberation of the Notch intracellular domain (N^{icd}) which forms a heteromeric transcriptional complex, and induces expression of Hes/Hey which act as transcriptional repressors¹⁹. Wnt ligand binds to LRP/Frizzled receptors resulting in sequestration of the APC/GSK/CK1 complex to the cell membrane, degradation of Ctnnb1 is prevented and Ctnnb1 is free to translocate to the cell nucleus where it binds Lef/Tcf transcription factors to enhancer elements of target genes²⁰⁻²². Notch signalling is modified by multiple factors including the ubiquitin ligase Numb which acts as a negative regulator of the Notch signalling pathway²³⁻²⁵. Numb is a direct transcriptional target of the Wnt signalling pathway and therefore represents a node at which these pathways can converge and interact during cell–fate determination^{26, 27}.

In ductular reactions of chronic human disease we sought to define Notch and Wnt signalling during lineage specification and have studied two disease patterns where ductular reactions form and human HPCs (hHPCs) are activated: We focused on Primary Biliary Cirrhosis (PBC) and Primary Sclerosing Cholangitis (PSC) when investigating biliary repair and Hepatitis C Virus (HCV) infection to investigate the mechanisms of hepatocellular regeneration. We modelled these disease states using mouse dietary regimes where a murine activated HPC niche forms and HPCs have been proven to contribute regeneration of hepatocytes and biliary epithelia^{3, 28}. We have utilised the Choline Deficient–Ethionine supplemented (CDE)^{29, 30} regime to model hepatocellular regeneration or 3,5–diethoxycarbonyl–1,4–dihydrocollidine (DDC)^{31, 32} to model biliary regeneration.

Results

Spatial variability in the HPC niche

HPC mediated liver regeneration is characterised by the emergence of a stereotypical inflammatory niche which forms around emerging HPCs³³. This activated HPC niche which constitutes the ductular reaction in human disease and murine models consists principally of macrophages and myofibroblasts and requires the *de novo* synthesis of ECM to facilitate

appropriate HPC expansion²⁹ (Fig. 1a). Using mouse models of both biliary and hepatocyte regeneration we have digitally reconstructed the activated murine HPC (mHPC) niche in 3-dimensions. We analysed serial sections for Macrophages (F4/80), Myofibroblasts (α SMA) HPCs (panCK) and Collagen-I from which we digitally reconstructed and assessed niche formation in these different regenerative contexts.

During biliary regeneration the activated mHPCs are surrounded by a thick layer of α SMA positive myofibroblasts, which constitutes the bulk of the activated ductular reaction, (Fig 1b) these myofibroblasts form close associations with the emerging HPCs and are therefore capable of influencing the mHPCs. Myofibroblasts are intimately associated with Collagen-I, which is deposited as a thick sheath around the ductular reaction (Fig 1c), and excludes macrophages from forming close associations with the mHPCs throughout biliary regeneration and we therefore hypothesise that macrophages are incapable of influencing mHPCs. During hepatocyte regeneration the mHPC niche consists predominantly of macrophages and is more diffuse with fewer myofibroblasts and reduced Collagen-I, allowing macrophages to associate closely with mHPCs. (Fig 1b,c).

Notch is involved in biliary regeneration

In both human biliary and hepatocellular diseases, *NOTCH1* and *NOTCH2* are highly expressed in Cytokeratin7 (Krt7) positive hHPCs isolated using laser-capture micro-dissection (Fig 2a). *NOTCH2* protein is found predominantly within the membrane and cytoplasm of hHPCs within the ductular reaction during hepatocyte regeneration (Fig 2a). In contrast, during biliary regeneration *NOTCH2* protein is frequently localised to the cytoplasm and nucleus of hHPCs, suggesting Notch pathway activation (Fig 2a). We confirmed the activation of the Notch pathway in end-stage biliary disease and regeneration by analysing the HES/HEY family of Notch targets. In biliary regeneration we saw high mRNA expression of both the Notch receptor targets *HES1* and *HEY1* (Fig 2a) when compared to those hHPCs isolated during hepatocyte regeneration, indicating that in hepatocyte regeneration there is restricted activation of the Notch pathway. In both human disease patterns the Notch receptors are expressed at high levels, however the Notch pathway ligand *JAGGED1* is modulated and expressed higher in the ductular reaction during biliary rather than hepatocyte regeneration. *JAGGED1* protein is consistently localised to the hHPC cell surface in PBC/PSC (Fig 2a) indicating active Notch signalling during biliary regeneration

To investigate the mechanisms underpinning these human observations we utilised murine models of mHPC derived hepatocellular and biliary regeneration. mHPCs were isolated using size and EpCAM positivity. In sorted mHPCs *Notch1* and *Notch2* are highly expressed during biliary regeneration compared to mHPCs isolated during hepatocellular regeneration (Fig 2b). Furthermore the Notch pathway effectors *Hes5* and *HeyL* are more highly expressed in mHPCs during biliary regeneration than hepatocyte regeneration (Fig 2b). Activation of the Notch signalling pathway was confirmed through visualisation of cleaved Notch1 in the nucleus of mHPCs during biliary regeneration, but was rarely seen in hepatocellular regeneration (Fig 2b) indicating these disease models appropriately reproduce the human Notch pathway paradigm. In murine biliary injury, *Jagged1* ligand is expressed by mHPC associated myofibroblasts whereas in hepatocellular injury *Jagged1* is not detectable in mHPC associated myofibroblasts (Fig 2b).

Notch inhibition results failure of biliary specification

We isolated mHPCs from mice with hepatocyte injury and co-cultured them with *Jagged1* positive myofibroblasts (Supplementary Fig 1a). This induced Notch pathway activation confirmed through induction of *Hes1* and *Hes5* as well as *Hey1* and *HeyL* and reflects the

Notch high state we describe during biliary regeneration (Supplementary Fig 1a). These co-cultures were treated either with DAPT (N-[N-(3,5-Difluorophenacetyl)-L-alanyl]-S-phenylglycine t-butyl ester), a γ -secretase (GS) inhibitor or vehicle alone. GS inhibition resulted in significant reduction in the expression of Notch effectors *Hes1*, *Hes5*, *Hey1* and *HeyL* (Fig 2c); The reduction in Hes/Hey gene expression is associated with an reduced expression of both the early transcription factor *Hnf1 β* and the mature biliary genes *Hnf6* and *Ggt* (Fig 2c).

Our *in vitro* data demonstrates that Notch signalling is required for the specification of HPCs into bile ducts. To demonstrate a functional role for Notch *in vivo* we blocked Notch receptor cleavage *in vivo* using DAPT as previously described^{34, 35}. Mice were given biliary damage for two weeks and received intravenous DAPT or control for the final five days of injury. GS inhibition resulted in a decreased number of mHPCs (Fig 2d). Isolated mHPCs demonstrated reduced expression of the Notch pathway effectors *Hes1* and *Hes5* from DAPT treated animals versus control. Furthermore *Hnf1 β* and *Hnf6* – genes associated with biliary phenotype, were reduced (Fig 2e). GS inhibition caused no change in the levels of the hepatocyte transcription factor *Hnf4a* (Fig 2e), suggesting that Notch signalling is not involved in hepatocyte regeneration. To confirm this we gave intravenous DAPT to mice undergoing two weeks of mHPC mediated hepatocyte regeneration and found no significant difference in the number of mHPCs versus controls. Moreover isolated mHPCs showed no change in expression of early liver enriched transcription factors *Hnf1 β* , *Hnf6* and *Hnf4a* versus controls (Supplementary Fig 1b). DAPT had no effect upon the niche composition or fibrosis indicating that loss of mHPCs is likely due to a differentiation defect, rather than a failure of mHPC maintenance by the surrounding activated niche (Supplementary Fig 2a–c).

Numb facilitates hepatocyte differentiation

Notch receptor is present in the ductular reactions of both human disease patterns and to a lesser degree during murine regeneration; we hypothesise that there was a second tier of Notch receptor inhibition. From our published array work we demonstrated an elevated expression of *NUMB* a post-transcriptional regulator of the Notch signalling pathway in HCV samples compared to PBC/PSC groups³⁶. In order to confirm the underlying factors which regulate Notch during hepatocellular and biliary regeneration we characterised *NUMB*. During hepatocellular regeneration hHPCs from the ductular reactions express *NUMB* at high levels in end-stage pathology. In contrast, *NUMB* is consistently lost within the ductular reactions during human biliary disease and regeneration; this is reflected in the levels of *NUMB* protein within the ductular reactions (Fig 3a). In the mouse models of hepatocellular regeneration we found a persistence of *Numb* protein throughout the biliary network and mHPCs over the two week time course we studied (Fig 3b). This was confirmed in isolated mHPCs where *Numb* was highly expressed. (Fig 3b). Induction of biliary regeneration results in a rapid loss of *Numb* from mHPCs at both the level of mRNA and protein (Fig 3b and Supplementary Fig 3a).

We used RNAi targeted to *Numb* in a well characterised mHPC line, BMOL³⁷, which becomes positive for *Hnf4a* and *Numb* when treated with canonical rhWnt3a (Fig 3c). Here we achieve a significant knockdown of *Numb* transcript levels using two sequences targeted to different domains of the *Numb* mRNA molecule (*Numb* RNAi1 (Fig 3d) and *Numb* RNAi2 (Supplementary Fig 3b)) compared to cells transfected with a scrambled RNAi control. *Numb* knockdown results in the activation of the *Hes1*, indicating that the Notch pathway has become activated, as well as increased *Hnf1 β* and *Hnf6* expression conferring biliary specification (Fig 3d).

Wnt drives hepatocyte differentiation *in vivo*

Stabilised CTNNB1 is found within the cytoplasm and nucleus of hHPC within ductular reactions of HCV infected liver, whereas in PBC/PSC CTNNB1 is predominantly localised to the cell surface, suggesting low activation of the canonical Wnt signalling pathway (Supplementary Fig 4a). We also observed comparable localisation of stable Ctnnb1 in our murine models of hepatocellular and biliary regeneration (Fig 4a). We confirmed this variation in Wnt pathway activation by expression analysis of the Wnt targets *Axin2*, *Sox9*, *Myc* and *Twist1*^{38, 39}. All of which are more highly expressed during hepatocellular than biliary regeneration (Fig 4a).

We used a transgenic mouse which expresses a Tamoxifen (TM) responsive Cre under the control of the Krt19 promoter (Krt19CreER^T)⁴⁰. We activated the canonical Wnt pathway by stabilising Ctnnb1 through conditional deletion of Exon3 (Ctnnb1^{ΔEx3}), making Ctnnb1 resistant to degradation and causing its nuclear accumulation (Fig 4b). All mice contained the Krt19 driven CreER^T and either a WT or ΔEx3 Ctnnb1 locus. Activation of the Ctnnb1 mutant and the subsequent accumulation of nuclear Ctnnb1 in mHPCs does not result in an increase in the number of Ctnnb1 high hepatocytes within the liver parenchyma when the mice are healthy (Fig 4c) indicating that the Cre line is not unselectively activated in adult hepatocytes and that activation of the Ctnnb1 mutant does not cause mHPCs to become hepatocytes in the absence of damage (Fig 4b). During two weeks of biliary damage there is only a small proportion of hepatocytes which demonstrate a high level of Ctnnb1 detected in the nucleus (approximately 3%) when Ctnnb1 is wild-type (Fig 4c). Upon TM administration to Krt19CreER^T/Ctnnb1^{ΔEx3} double transgenic mice the number of hepatocytes which are positive for nuclear Ctnnb1 increases significantly from approximately 3% to 12.5% (Fig 4c), indicating that during biliary damage, ectopic activation of the canonical Wnt pathway through stabilization of Ctnnb1 redirects mHPCs from a cholangiocytic fate into a hepatocellular one.

Bile ducts form in the absence of hepatic macrophages

Our data indicate that Wnt signalling is required for HPC specification into hepatocytes. To address the source of Wnt expression observed during regeneration of hepatocytes we isolated F4/80 positive macrophages from mice undergoing either biliary or hepatocyte regeneration. Macrophages from animals undergoing hepatocyte regeneration express high levels of *Wnt3a* (Fig 5a); during biliary regeneration expression of *Wnt3a* is reduced compared with control animals (Fig 5a). The Wnt3a protein can be readily seen as punctuate positivity in mononuclear cells in the activated niche forming close associations with panCK positive mHPCs during hepatocyte regeneration (Fig 5a). Wnt3a positive cells are only found very infrequently associated with mHPCs during biliary regeneration, where they are restricted to the inflammatory region, outwith the myofibroblast niche (Supplementary Fig 4b).

The interaction of macrophages with hepatocyte debris induces Wnt expression. We exposed murine bone-marrow derived macrophages to sonicated hepatocyte debris. Phagocytosis of this resulted in the upregulation of both canonical ligands *Wnt3a* and *Wnt7a* (Fig 5b); this phenotype is induced only through the phagocytosis of biological debris, and not synthetic phagocytic substrates (latex beads or liposomes)⁴¹. Co-culture of post-phagocytic macrophages with primary mHPCs *in vitro* results in an increased expression of Wnt target genes in these direct co-cultures which are not expressed in the single cultures alone (Supplementary Fig 4d). Treatment of these co-cultures with the Wnt inhibitor rhWIF1 results in a significant reduction in the expression of Wnt pathway targets *Axin2*, *Myc*, *Sox9* and *Twist1*. Moreover treatment of the mHPC/macrophage co-cultures with rhWIF1 resulted in the reduced expression of the hepatocyte genes *Hnf4a* and *Hnf1a* whilst

promoting the expression of biliary genes *Hnf1β* and *Hnf6*, suggesting that *in vitro* macrophage derived Wnt is important in the maintenance of hepatocyte phenotype and the suppression of biliary differentiation (Fig 5c). In this co-culture system it is possible that activation of the canonical Wnt targets is also occurring in macrophages however as macrophages do not express liver enriched transcription factors (Supplementary Fig 4e), we can conclude that the canonical Wnt pathway promotes hepatocyte specification within the mHPCs; to confirm this we decided to remove macrophages during mHPC mediated regeneration and address whether canonical Wnt targets and mHPC phenotype is altered *in vivo*.

We ablated liver macrophages using liposomal clodronate⁴² every three days during two weeks hepatocellular injury and regeneration which was confirmed as the pan-macrophage marker F4/80 was lost following clodronate but not in controls (Supplementary Fig 5a). Liposomal clodronate did not have off target effects and the remainder of the non-parenchymal cells remain intact during regeneration (Supplementary Fig 5b). Ablation of macrophages during hepatocyte regeneration resulted in mHPCs forming peri-portal biliary structures with a clear lumen akin to bile ducts rather than infiltrating the parenchyma to regenerate hepatocytes (Fig 6a). There was no nuclear Ctnnb1 seen in mHPCs of macrophages depleted animals, whereas in controls Ctnnb1 localises to the mHPC nucleus, implying activation of the canonical Wnt pathway (Fig 6a and Supplementary Fig 6a). During macrophage ablation the levels Wnt pathway targets *Axin2*, *Myc*, *Sox9* and *Twist1* in mHPCs are decreased versus controls suggesting that macrophage ablation results in a loss of the canonical Wnt signalling to mHPCs (Fig 6b). The promoter region of *Numb* contains TCF/LEF binding sites and may be directly regulated through the canonical Wnt signalling pathway²⁶. During macrophage ablation the levels of *Numb* transcript fall significantly, moreover macrophage ablation during hepatocellular regeneration results in loss of the hepatocyte transcription factors *Hnf4a* and *Hnf1a* whilst inducing the expression of *Hes1*, as well as the biliary genes *Hnf1β* and *Hnf6* indicating that in the absence of macrophages, mHPCs form bile ducts as a default lineage pathway and exit from this fate occurs in a Wnt dependent manner (Supplementary Fig 6b). Ultimately ablation of macrophages results in an increase in the number of *Hnf1β* positive mHPCs (Fig 6c) and a reduction in the number *Hnf4a* positive mHPCs (Fig 6c).

Discussion

Here we describe for the first time the mechanisms by which HPCs in the adult liver are able to acquire divergent cell fates in response to diverse disease and how the local cellular microenvironment can be modulated to achieve a defined progenitor specification. Notch signalling has been described in the ontogeny of bile ducts from an equipotent population of foetal hepatoblasts⁴³, abrogation of which results in the biliary malformations seen in Alagilles syndrome⁴⁴. Here, we observe that during adult biliary regeneration there is a requirement for an activated Notch signalling pathway in order to specify biliary epithelium from naïve HPCs, and that in the mouse there is a recapitulation of the portal mesenchyme seen during development⁴⁵. We found Jagged1 ligand in close proximity to Notch receptor on the HPCs, which express higher levels of Notch signalling pathway targets *Hes* and *Hey* during biliary regeneration. *In vitro* and *in vivo* inhibition of Notch signalling demonstrates that Notch is required for adult biliary specification, with a reduction *in vivo* of biliary cell numbers and liver enriched transcription factors associated with biliary fate^{46, 47}.

We describe a canonical Wnt dependent action for the ubiquitin ligase *Numb*, which is required for the exit of HPCs from a biliary specification and acquisition of a hepatocyte cellular fate. In a mHPC cell line stimulation with canonical Wnt3a, a ligand implicated in multiple stages of hepatocyte differentiation⁴⁸, drives *Numb* expression. Moreover

inhibition of Numb facilitates the activation of the Notch signalling, as previously described^{49, 50} and activates a biliary phenotype. This study has identified a novel role for the canonical Wnt signalling pathway in mHPC specification to hepatocytes *in vivo*, where ectopic activation of the Wnt pathway commits mHPCs to a hepatocyte fate (summarised in Supplementary Fig 7). Importantly this data demonstrates that interactions between pathways are critical for correct HPC specification. Other signalling pathways may also be implicated in HPC specification. Sox9 is a mHPC marker^{3, 28}. Sox9 is regulated by both canonical Wnt signalling and Hedgehog (Hh) signalling⁵¹; the latter also acting as a modifier of the canonical Wnt pathway⁵². Hh signalling has also been extensively implicated in the phenotype of Alagilles Syndrome and has a critical role in biliary remodelling^{53, 54} indicating that there may be a node at which the Hh/Wnt/Notch could interact in order to regulate the relationship between HPC proliferation and fate.⁵⁵

The inflammatory stroma has been understudied as a component of the hepatic regenerative response however the pathological analysis of other organs considers this a key component of regeneration. In kidney regeneration macrophage derived Wnt7b is required for renal tubular epithelial regeneration^{7, 56}. In liver disease the hepatic immune component has been demonstrated to play a critical role in the survival and maintenance of hepatocytes^{57, 58}. Here we describe how hepatic macrophages play a role in HPC mediated regeneration of hepatocytes where Wnt3a is expressed by macrophages as a result of the phagocytosis of biological debris, implicating macrophages in environmental sensing and correct epithelial repair from HPCs⁵⁹. Animals which lack macrophages *in vivo* fail to specify hepatocytes from mHPCs, their mHPCs up-regulate biliary genes, fail to migrate and form aberrant tubules, akin to regeneration during biliary disease⁶⁰. In severe liver disease marked ductular reactions and failure of adequate hepatocyte regeneration is often seen. Understanding the biology of this may open a therapeutic target to stimulate healthy regeneration.

Methods

Animal Work

8 week-old male wild-type C57B16, S129S2/SvHsd mice from Harlan UK or Krt19CreER^T/Ctnnb1^{ΔEx3} mice were held under specific-pathogen-free conditions in 12h light/dark cycles. C57B16 mice were fed on Choline-Deficient diet (MP Biomedicals) for upto 2 weeks and water supplemented with 0.15% w/v DL-Ethionine (Sigma). S129S2/SvHsd mice were treated 3, 5-diethoxycarbonyl-1, 4-dihydrocollidine (DDC) (0.1% Purina 5015 mouse chow) for upto 14 days. Cre expressing animals were induced with 1 IP injection of TM at 80mg kg⁻¹ at day 5 of the experiment. All experimental procedures were approved by the UK home office.

mHPC culture

Livers were minced in Leibovitz-15 containing Collagenase B and DNase I and passed through a 40μm cell strainer (BD falcon). Cells were centrifuged over a discontinuous Percoll gradient and cultured as previously described³⁷. For co-cultures 5×10⁵ mHPCs were co-cultured with 1×10⁵ myofibroblasts/macrophages in differentiation medium³³. DAPT (Tocris) used at 10mM. rhWIF-1 (R&D Biosciences) used at 250ng ml⁻¹. hrWnt3a (Peprotech) used at a concentration of 30ug ml⁻¹ and co-cultured for 3 days. BMDMs were generated from the bone-marrow of wildtype mice cultured in DMEM supplemented with L929 conditioned medium in low adhesion flasks (Corning). Myofibroblasts for the co-culture studies were isolated from healthy murine livers and separated based on density using Ficoll-Paque (GE lifesciences); cells were plated on plastic and allowed to activate in DMEM containing 10% FCS.

Immunohistochemistry

Formalin or methacarn fixed tissue was cut to 5 μ m. Sections were antigen retrieved with sodium citrate. Sections were blocked using H₂O₂ (Sigma), followed by Avidin/Biotin blocking and species specific serum (Dako). Primary antibodies were incubated overnight (panCK #Z0622 (Dako), Dlk-1 #ab21682, NUMB #14140, EpCam #32392, F4/80 #ab6640 (Abcam); Jagged1 #sc-8303, Notch1 #sc-6014, Notch2 #sc-7423, Hnf4 α #sc-6556 and Hnf1 β #sc-7411 (Santa Cruz Biotechnology) Wnt3a #09-162 (Millipore), α SMA #BMK-2202 (Vector) Collagen-I. Species specific anti-IgG biotinylated antibodies (DAKO) were used for detection. ABC HRP detection kit was supplied by Vector. DAB substrate was supplied by DAKO or alternatively fluorescent conjugated secondary antibodies (Alexa555/Alexa568 and Alexa488) were used (all from Invitrogen). All photographs were taken using a Nikon Eclipse e600 microscope and camera (DXM1200F) and acquired using NIS-Elements D software (Nikon)

FACS separation of mHPCs: Cells were incubated with 40 μ g ml⁻¹ EpCam antibody (clone G8.8) Biolegend #118211 and sorted using a FACS Diva (Becton Dickinson and Co.).

qPCR Preparation and Analysis

RNA was using Trizol reagent (Amersham). Precipitated RNA was applied to an RNAmi spin column (Qiagen) and prepared according to manufacturer's instructions. RNA was reverse transcribed using QuantiTect reverse transcription kit (Qiagen). Gene expression analysis was achieved using pre-validated QuantiTect primers with Quantifast SYBR reagent (Qiagen).

Macrophage ablation

200 μ l of clodronate liposomes or control PBS were injected I.V. for the duration of CDE treatment. Liposomes contained Phosphatidylcholine (LIPOID E PC) obtained from Lipoid GmbH, Ludwigshafen, Germany. Cholesterol is purchased from Sigma

Image analysis

Adjacent, non-overlapping images were taken from three lobes in treated vs. control mice (n=45 per mouse). All images had a matched exposure time and light intensity. Control mice were used to establish parameters for image analysis. Data is represented as function of positive pixels over total pixels per field.

Human Work

Human biopsies were obtained from explants livers of patient with end-stage liver disease. The diagnosis is based on clinical and radiological data, and confirmed by histology (Supplementary Fig 8). Several aetiologies were included: The use of human tissues for this study was approved by the Local Commission for Medical Ethics of the University of Leuven. 10 μ m frozen sections of human liver biopsies (chronic hepatitis C: n=6, primary biliary cirrhosis: n=6, primary sclerosing cholangitis: n=4) and LCM was performed as previously described³⁴.

Quantitative PCR

Total RNA was extracted from microdissected samples using Arcturus PicoPure RNA Isolation kit (Applied Biosystems) according to the manufacturer's instruction. RNA quality after LCM was determined with an Agilent BioAnalyzer-2100 (Agilent) in combination with RNA 6000 Pico-LabChip. The RNA was amplified with the WT-Ovation™ Pico RNA Amplification System (NuGEN Technologies)³⁴. The amplified product was purified with DNA Clean&Concentrator™-25 kits from Zymo research (Baseclear Lab Products).qPCR

experiments were conducted on an ABI PRISM 7900 sequence detector system (Applied Biosystems) with predesigned primers and RT2 Real-Time SYBR Green/Fluorescein master mix (SABiosciences), according to the manufacturer's instruction. Reference genes: 18s ribosomal RNA, hypoxanthine phosphoribosyltransferase 1, ribosomal protein L13a, ribosomal protein L19, glyceraldehyde 3-phosphate dehydrogenase and β -actin.

Immunohistochemistry

for KRT19, NOTCH1, NOTCH2, NUMB, JAGGED1 CTNNA1 was performed on serial paraffin sections. 5 μ m sections were used. Target retrieval was performed with EnVision™ FLEX Target Retrieval Solution (Dako, Denmark). Endogenous peroxidase activity was blocked using EnVision™ Peroxidase-Blocking Reagent (Dako). Sections were incubated with primary antibody. Subsequently, the slides were further processed using the EnVision™ Dual Link (Dako) against primary species. The complex was visualized with DAB (Dako) Using Leica DC300 camera with the software IM50 Image Manager from Leica. Statistical Analysis We performed statistical analyses with GraphPad v3.0. We used the Mann-Whitney test to evaluate differences between treatments due to non-normal distribution of the data. All analysis was two-tailed. In all cases, $P < 0.05$ was considered significant.

Supplementary Material

Refer to Web version on PubMed Central for supplementary material.

Acknowledgments

Cl₂MDP (or clodronate) was a gift of Roche Diagnostics GmbH, Mannheim, Germany. Thanks to R Aucott for the donation of murine hepatic fibroblasts. SJF is supported by the Medical Research Council, Sir Jules Thorn Trust and Wellcome Trust, LGB is funded through an MRC project grant and was funded through an MRC studentship.

Reference List

1. World Health Organisation. Disease and injury country estimates, Burden of disease. 2009. http://www.who.int/healthinfo/global_burden_disease/estimates_country/en/index.html. Ref Type: Generic
2. Hay DC. Cadaveric hepatocytes repopulate diseased livers: life after death. *Gastroenterology*. 2010; 139:729–731. [PubMed: 20659459]
3. Furuyama K, et al. Continuous cell supply from a Sox9-expressing progenitor zone in adult liver, exocrine pancreas and intestine. *Nat Genet*. 2010
4. Fellous TG, et al. Locating the stem cell niche and tracing hepatocyte lineages in human liver. *Hepatology*. 2009; 49:1655–1663. [PubMed: 19309719]
5. Gouw AS, Clouston AD, Theise ND. Ductular reactions in human liver: Diversity at the interface. *Hepatology*. 2011; 54:1853–1863. [PubMed: 21983984]
6. Fallowfield JA, et al. Scar-associated macrophages are a major source of hepatic matrix metalloproteinase-13 and facilitate the resolution of murine hepatic fibrosis. *J Immunol*. 2007; 178:5288–5295. [PubMed: 17404313]
7. Lin SL, et al. Macrophage Wnt7b is critical for kidney repair and regeneration. *Proc Natl Acad Sci U S A*. 2010; 107:4194–4199. [PubMed: 20160075]
8. Duffield JS, et al. Selective depletion of macrophages reveals distinct, opposing roles during liver injury and repair. *J. Clin. Invest*. 2005; 115:56–65. [PubMed: 15630444]
9. Tanimizu N, Miyajima A. Notch signaling controls hepatoblast differentiation by altering the expression of liver-enriched transcription factors. *J Cell Sci*. 2004; 117:3165–3174. [PubMed: 15226394]
10. Goessling W, et al. APC mutant zebrafish uncover a changing temporal requirement for wnt signaling in liver development. *Dev Biol*. 2008; 320:161–174. [PubMed: 18585699]

11. Burke ZD, et al. Liver zonation occurs through a beta-catenin-dependent, c-Myc-independent mechanism. *Gastroenterology*. 2009; 136:2316–2324. [PubMed: 19268669]
12. Lozier J, McCright B, Gridley T. Notch signaling regulates bile duct morphogenesis in mice. *PLoS ONE*. 2008; 3
13. McCright B, Lozier J, Gridley T. A mouse model of Alagille syndrome: Notch2 as a genetic modifier of Jag1 haploinsufficiency. *Development*. 2002; 129:1075–1082. [PubMed: 11861489]
14. Oda T, et al. Mutations in the human Jagged1 gene are responsible for Alagille syndrome. *Nat Genet*. 1997; 16:235–242. [PubMed: 9207787]
15. Li L, et al. Alagille syndrome is caused by mutations in human Jagged1, which encodes a ligand for Notch1. *Nat Genet*. 1997; 16:243–251. [PubMed: 9207788]
16. McDaniell R, et al. NOTCH2 mutations cause Alagille syndrome, a heterogeneous disorder of the notch signaling pathway. *Am J Hum Genet*. 2006; 79:169–173. [PubMed: 16773578]
17. Sparks EE, Huppert KA, Brown MA, Washington MK, Huppert SS. Notch signaling regulates formation of the three-dimensional architecture of intrahepatic bile ducts in mice. *Hepatology*. 2010; 51:1391–1400. [PubMed: 20069650]
18. Bray SJ. Notch signalling: a simple pathway becomes complex. *Nat Rev Mol Cell Biol*. 2006; 7:678–689. [PubMed: 16921404]
19. Iso T, Kedes L, Hamamori Y. HES and HERP families: multiple effectors of the Notch signaling pathway. *J Cell Physiol*. 2003; 194:237–255. [PubMed: 12548545]
20. Lee YJ, Swencki B, Shoichet S, Shivdasani RA. A possible role for the high mobility group box transcription factor Tcf-4 in vertebrate gut epithelial cell differentiation. *J Biol Chem*. 1999; 274:1566–1572. [PubMed: 9880534]
21. Okamura RM, et al. Redundant regulation of T cell differentiation and TCRalpha gene expression by the transcription factors LEF-1 and TCF-1. *Immunity*. 1998; 8:11–20. [PubMed: 9462507]
22. van HL, et al. The sequence-specific high mobility group 1 box of TCF-1 adopts a predominantly alpha-helical conformation in solution. *J Biol Chem*. 1993; 268:18083–18087. [PubMed: 8349685]
23. McGill MA, Dho SE, Weinmaster G, McGlade CJ. Numb regulates post-endocytic trafficking and degradation of Notch1. *J Biol Chem*. 2009; 284:26427–26438. [PubMed: 19567869]
24. McGill MA, McGlade CJ. Mammalian numb proteins promote Notch1 receptor ubiquitination and degradation of the Notch1 intracellular domain. *J Biol Chem*. 2003; 278:23196–23203. [PubMed: 12682059]
25. Spana EP, Doe CQ. Numb antagonizes Notch signaling to specify sibling neuron cell fates. *Neuron*. 1996; 17:21–26.
26. Katoh M, Katoh M. NUMB is a break of WNT-Notch signaling cycle. *Int J Mol Med*. 2006; 18:517–521. [PubMed: 16865239]
27. Cheng X, Huber TL, Chen VC, Gadue P, Keller GM. Numb mediates the interaction between Wnt and Notch to modulate primitive erythropoietic specification from the hemangioblast. *Development*. 2008; 135:3447–3458. [PubMed: 18799543]
28. Cardinale V, et al. Multipotent stem/progenitor cells in human biliary tree give rise to hepatocytes, cholangiocytes and pancreatic islets. *Hepatology*. 2011
29. Van Hul NK, barca-Quinones J, Sempoux C, Horsmans Y, Leclercq IA. Relation between liver progenitor cell expansion and extracellular matrix deposition in a CDE-induced murine model of chronic liver injury. *Hepatology*. 2009; 49:1625–1635. [PubMed: 19296469]
30. Akhurst B, et al. A modified choline-deficient, ethionine-supplemented diet protocol effectively induces oval cells in mouse liver. *Hepatology*. 2001; 34:519–522. [PubMed: 11526537]
31. Wang X, et al. The origin and liver repopulating capacity of murine oval cells. *Proc Natl Acad Sci U S A*. 2003; 100(Suppl 1):11881–11888. [PubMed: 12902545]
32. Fickert P, et al. A new xenobiotic-induced mouse model of sclerosing cholangitis and biliary fibrosis. *Am J Pathol*. 2007; 171:525–536. [PubMed: 17600122]
33. Lorenzini S, et al. Characterisation of a stereotypical cellular and extracellular adult liver progenitor cell niche in rodents and diseased human liver. *Gut*. 2010; 59:645–654. [PubMed: 20427399]

34. van Es JH, et al. Notch/gamma-secretase inhibition turns proliferative cells in intestinal crypts and adenomas into goblet cells. *Nature* 2005; 435:959–963.
35. Hellstrom M, et al. Dll4 signalling through Notch1 regulates formation of tip cells during angiogenesis. *Nature*. 2007; 445:776–780. [PubMed: 17259973]
36. Spee B, et al. Characterisation of the liver progenitor cell niche in liver diseases: potential involvement of Wnt and Notch signalling. *Gut*. 2010; 59:247–257. [PubMed: 19880964]
37. Tirmitz-Parker JE, Tonkin JN, Knight B, Olynyk JK, Yeoh GC. Isolation, culture and immortalisation of hepatic oval cells from adult mice fed a choline-deficient, ethionine-supplemented diet. *Int J Biochem Cell Biol*. 2007; 39:2226–2239. [PubMed: 17693121]
38. Lustig B, et al. Negative feedback loop of Wnt signaling through upregulation of conductin/axin2 in colorectal and liver tumors. *Mol Cell Biol*. 2002; 22:1184–1193. [PubMed: 11809809]
39. Mori-Akiyama Y, et al. SOX9 is required for the differentiation of paneth cells in the intestinal epithelium. *Gastroenterology*. 2007; 133:539–546. [PubMed: 17681175]
40. Means AL, Xu Y, Zhao A, Ray KC, Gu G. A CK19(CreERT) knockin mouse line allows for conditional DNA recombination in epithelial cells in multiple endodermal organs. *Genesis*. 2008; 46:318–323. [PubMed: 18543299]
41. Chung EY, Kim SJ, Ma XJ. Regulation of cytokine production during phagocytosis of apoptotic cells. *Cell Res*. 2006; 16:154–161. [PubMed: 16474428]
42. Van RN, Sanders A. Kupffer cell depletion by liposome-delivered drugs: comparative activity of intracellular clodronate, propamidine, and ethylenediaminetetraacetic acid. *Hepatology*. 1996; 23:1239–1243. [PubMed: 8621159]
43. Lemaigre FP. Notch signaling in bile duct development: new insights raise new questions. *Hepatology*. 2008; 48:358–360. [PubMed: 18666255]
44. Crosnier C, et al. JAGGED1 gene expression during human embryogenesis elucidates the wide phenotypic spectrum of Alagille syndrome. *Hepatology*. 2000; 32:574–581. [PubMed: 10960452]
45. Hofmann JJ, et al. Jagged1 in the portal vein mesenchyme regulates intrahepatic bile duct development: insights into Alagille syndrome. *Development*. 2010; 137:4061–4072. [PubMed: 21062863]
46. Yamasaki H, et al. Suppression of C/EBPalpha expression in periportal hepatoblasts may stimulate biliary cell differentiation through increased Hnf6 and Hnf1b expression. *Development*. 2006; 133:4233–4243. [PubMed: 17021047]
47. Clotman F, et al. The oncut transcription factor HNF6 is required for normal development of the biliary tract. *Development*. 2002; 129:1819–1828. [PubMed: 11934848]
48. Fletcher J, et al. The inhibitory role of stromal cell mesenchyme on human embryonic stem cell hepatocyte differentiation is overcome by Wnt3a treatment. *Cloning Stem Cells*. 2008; 10:331–339. [PubMed: 18479212]
49. Frise E, Knoblich JA, Younger-Shepherd S, Jan LY, Jan YN. The Drosophila Numb protein inhibits signaling of the Notch receptor during cell-cell interaction in sensory organ lineage. *Proc Natl Acad Sci U S A*. 1996; 93:11925–11932. [PubMed: 8876239]
50. McGill MA, McGlade CJ. Mammalian numb proteins promote Notch1 receptor ubiquitination and degradation of the Notch1 intracellular domain. *J Biol Chem*. 2003; 278:23196–23203. [PubMed: 12682059]
51. Park J, et al. Regulation of Sox9 by Sonic Hedgehog (Shh) is essential for patterning and formation of tracheal cartilage. *Dev. Dyn*. 2010; 239:514–526. [PubMed: 20034104]
52. Glise B, Jones DL, Ingham PW. Notch and Wingless modulate the response of cells to Hedgehog signalling in the Drosophila wing. *Dev. Biol*. 2002; 248:93–106. [PubMed: 12142023]
53. Omenetti A, et al. The hedgehog pathway regulates remodelling responses to biliary obstruction in rats. *Gut*. 2008; 57:1275–1282. [PubMed: 18375471]
54. Omenetti A, Diehl AM. Hedgehog signaling in cholangiocytes. *Curr. Opin. Gastroenterol*. 2011; 27:268–275. [PubMed: 21423008]
55. Choi SS, Omenetti A, Syn WK, Diehl AM. The role of Hedgehog signaling in fibrogenic liver repair. *Int. J. Biochem. Cell Biol*. 2011; 43:238–244. [PubMed: 21056686]

56. Karner CM, et al. Wnt9b signaling regulates planar cell polarity and kidney tubule morphogenesis. *Nat Genet.* 2009; 41:793–799. [PubMed: 19543268]
57. Polakos NK, et al. Kupffer cell-dependent hepatitis occurs during influenza infection. *Am. J. Pathol.* 2006; 168:1169–1178. [PubMed: 16565492]
58. Klein I, et al. Kupffer cell heterogeneity: functional properties of bone marrow derived and sessile hepatic macrophages. *Blood.* 2007; 110:4077–4085. [PubMed: 17690256]
59. Reddy SM, et al. Phagocytosis of apoptotic cells by macrophages induces novel signaling events leading to cytokine-independent survival and inhibition of proliferation: activation of Akt and inhibition of extracellular signal-regulated kinases 1 and 2. *J Immunol.* 2002; 169:702–713. [PubMed: 12097372]
60. Nijjar SS, Crosby HA, Wallace L, Hubscher SG, Strain AJ. Notch receptor expression in adult human liver: a possible role in bile duct formation and hepatic neovascularization. *Hepatology.* 2001; 34:1184–1192. [PubMed: 11732008]

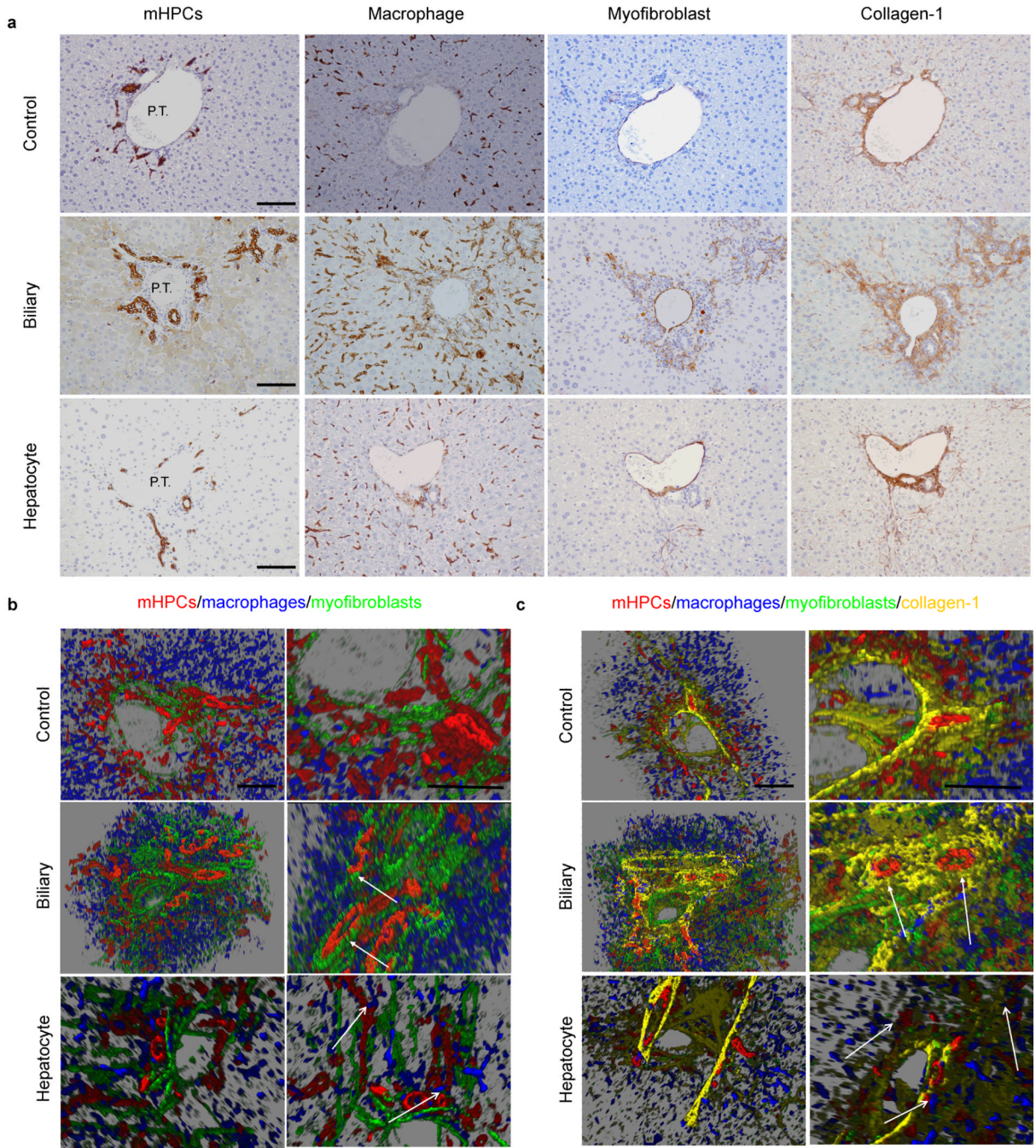


Figure 1. Spatial regulation of the HPC niche is dependent on adult disease pattern
(a) Upper photomicrographs: Healthy adult liver with panCK positive mHPCs, F4/80 positive macrophages, α SMA positive myfibroblasts with collagen-1 surrounding the vasculature. In biliary regeneration (middle photomicrographs) α SMA positive myfibroblasts, as well as collagen-I surround mHPCs, F4/80 macrophages around the PT but not associated with the mHPCs. During hepatocellular (lower photomicrographs) damage mHPCs are associated with both F4/80 positive macrophages and diffuse α SMA positive myfibroblasts, with little collagen deposition around the mHPCs. **(b)** 3D reconstruction of the mHPC niche. mHPCs (red, denoted with white arrows) expand as

pseudo-ducts or chords of mHPCs in biliary and hepatocyte regeneration respectively. In biliary regeneration mHPCs are closely associated with myofibroblasts (green) close to the portal tract between the mHPCs and macrophages (blue). During hepatocyte regeneration there is little association of myofibroblasts (green) and mHPCs (red), macrophages (blue) are closely associated with mHPCs. (c) Addition of collagen-I to the 3-D constructs reveals that there is an extracellular barrier between mHPCs and macrophages that is more prominent during biliary injury and regeneration than hepatocellular injury and regeneration.

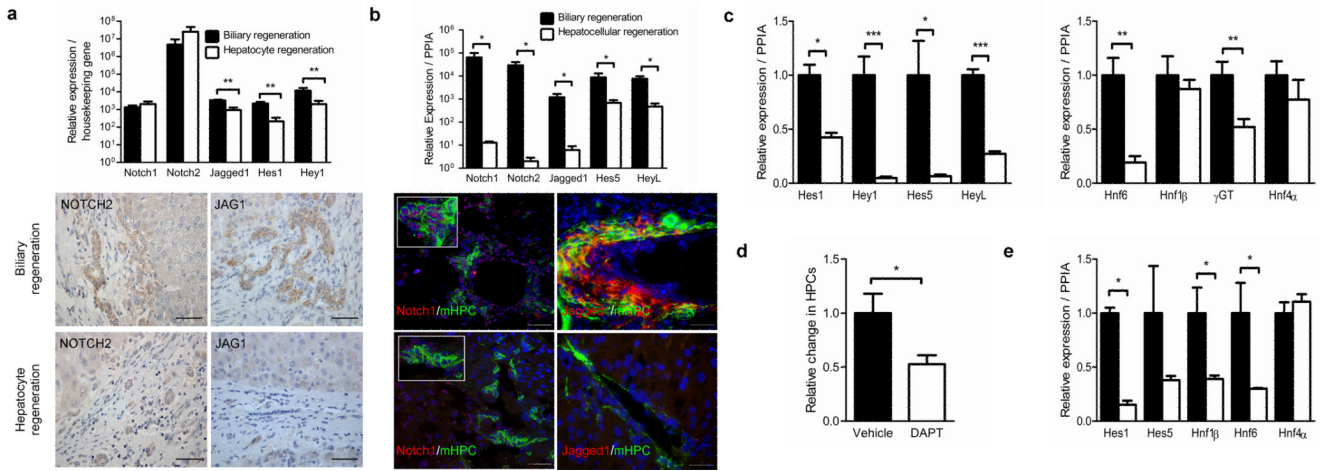


Figure 2. Modulation of the Notch pathway *in vitro* and *in vivo* affects biliary regeneration (a) mRNA expression of the NOTCH signalling pathway components in isolated ductular reactions of both hepatocellular and biliary patterns of disease. Immunohistochemistry for NOTCH2 and JAGGED1 with positivity during biliary disease (upper photomicrographs), however in hepatocellular regeneration only NOTCH2 protein is detectable (lower photomicrographs). (b) Notch pathway expression in murine models of biliary (upper photomicrographs) and hepatocellular (lower photomicrographs) regeneration; Notch1 protein (red) in the EpCAM positive biliary tree (green) and Jagged1 (red) in the surrounding ductular stromal α SMA positive fibroblasts (green). (c) mRNA expression of Notch targets and liver enriched transcription factors after inhibition of the Notch pathway with DAPT in direct co-cultures of mHPCs and myofibroblasts *in vitro* (d) Quantification of absolute mHPC numbers in animals treated with DAPT *in vivo* vs. vehicle alone control. (e) Expression of Notch pathway targets and liver enriched transcription factors in mHPCs isolated from DAPT treated animals vs. vehicle alone controls. Data is expressed as means \pm S.E.M; * $P < 0.05$, ** $P < 0.01$, *** $P < 0.001$. Human: PBC/PSC $n = 10$ HCV $n = 6$. Murine CDE $n = 4$ DDC $n = 4$. Scale bar = 50 μ m

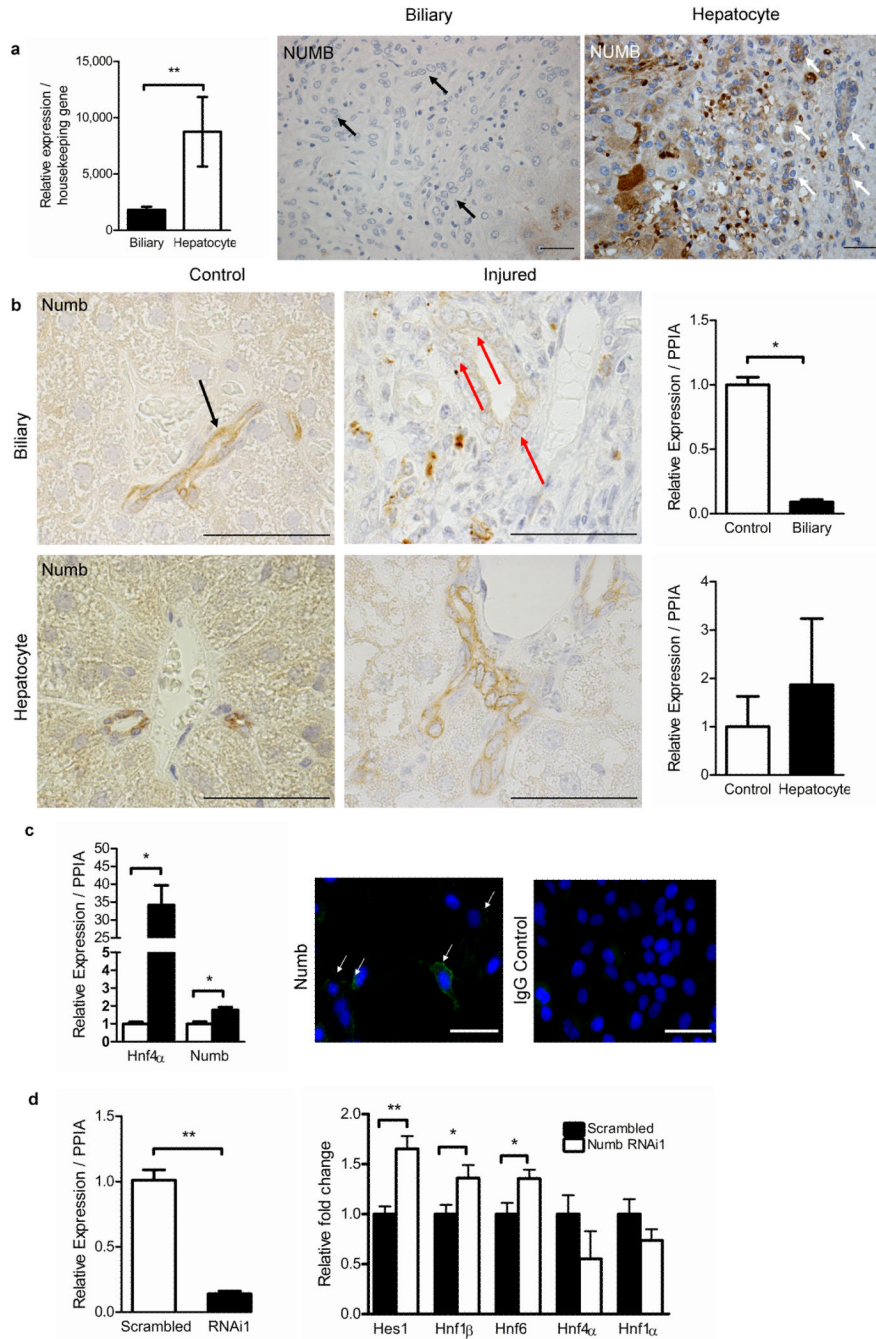


Figure 3. Numb represses the Notch signalling pathway and allows hepatocyte differentiation (a) NUMB mRNA expression and presence (white arrows) or absence (black arrows) of NUMB protein in human ductular reactions isolated from HCV or PSC/PBC disease patterns. (b) Expression of murine Numb protein in healthy liver and during hepatocyte regeneration (black arrows) the loss of Numb in mHPCs during biliary regeneration is highlighted (red arrows); these changes are reflected in Numb mRNA expression levels from isolated mHPCs. (c) Expression levels of Hnf4α and Numb in isolated mHPCs when stimulated with Wnt3a *in vitro*. The Numb protein (green) can be identified in the mHPC BMOL cell line using immunohistochemistry. (d) Expression of Numb, Notch pathway

targets and liver enriched transcription factors in response to Numb RNAi, a similar affect is seen using a second independent Numb sequence (Supplementary Fig 3b). Data is expressed as means \pm S.E.M; * $P < 0.05$, ** $P < 0.01$, *** $P < 0.001$. Human: PBC/PSC $n = 10$ HCV $n = 6$. Murine CDE $n = 4$ DDC $n = 4$. Scale bar = $50\mu\text{m}$. *In vitro* $n = 12$.

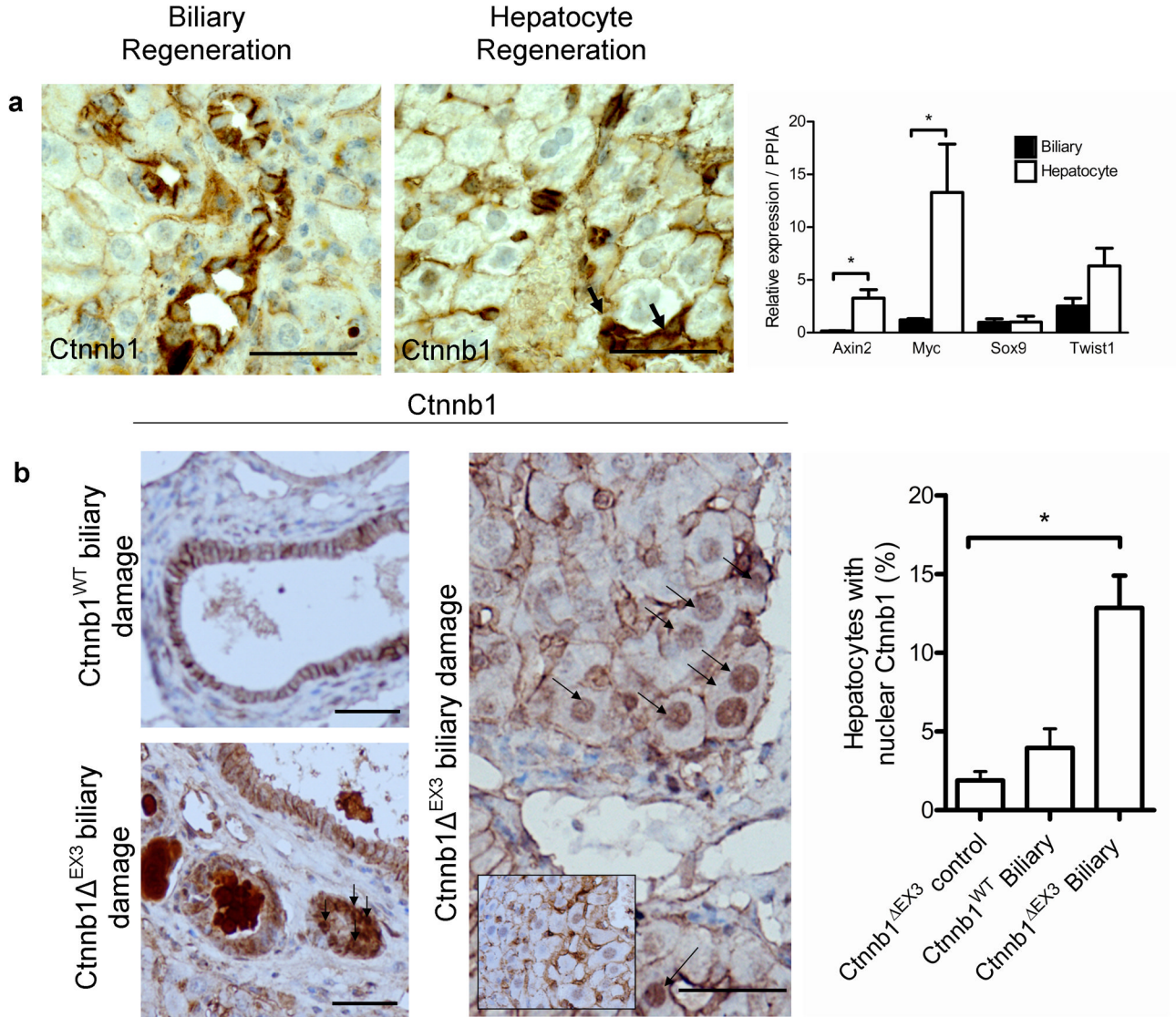


Figure 4. The Wnt pathway drives exit of mHPCs from a biliary fate into a hepatocyte phenotype

(a) Photomicrographs demonstrating immunohistochemistry for nuclear Ctnnb1 in mHPCs during hepatocellular and biliary regeneration. Relative expression of canonical Wnt targets Axin2, Myc, Sox9 and Twist1 in mHPCs from hepatocellular vs. biliary regeneration. (b) Immunohistochemistry for stabilized Ctnnb1 (black arrows) in Krt19–Cre expressing cells harbouring the Ctnnb1^{ΔEx3} or Ctnnb1^{WT} locus. Central photomicrographs showing nuclear Ctnnb1 in hepatocytes of Ctnnb1^{ΔEx3} mutants or Ctnnb1^{WT} (inset image) after biliary damage; Quantification of hepatocytes with nuclear Ctnnb1 in animals harbouring the Ctnnb1^{ΔEx3} vs. Ctnnb1^{WT}. Data is expressed as means ± S.E.M; **P* < 0.05, ***P* < 0.01, ****P* < 0.001. CDE *n* = 4 DDC *n* = 4, Wnt3a treated HPCs *n* = 6, Fed BMDMs *n* = 6, LRP5/6 *n* = 4 – 6. Scale bar = 50μm

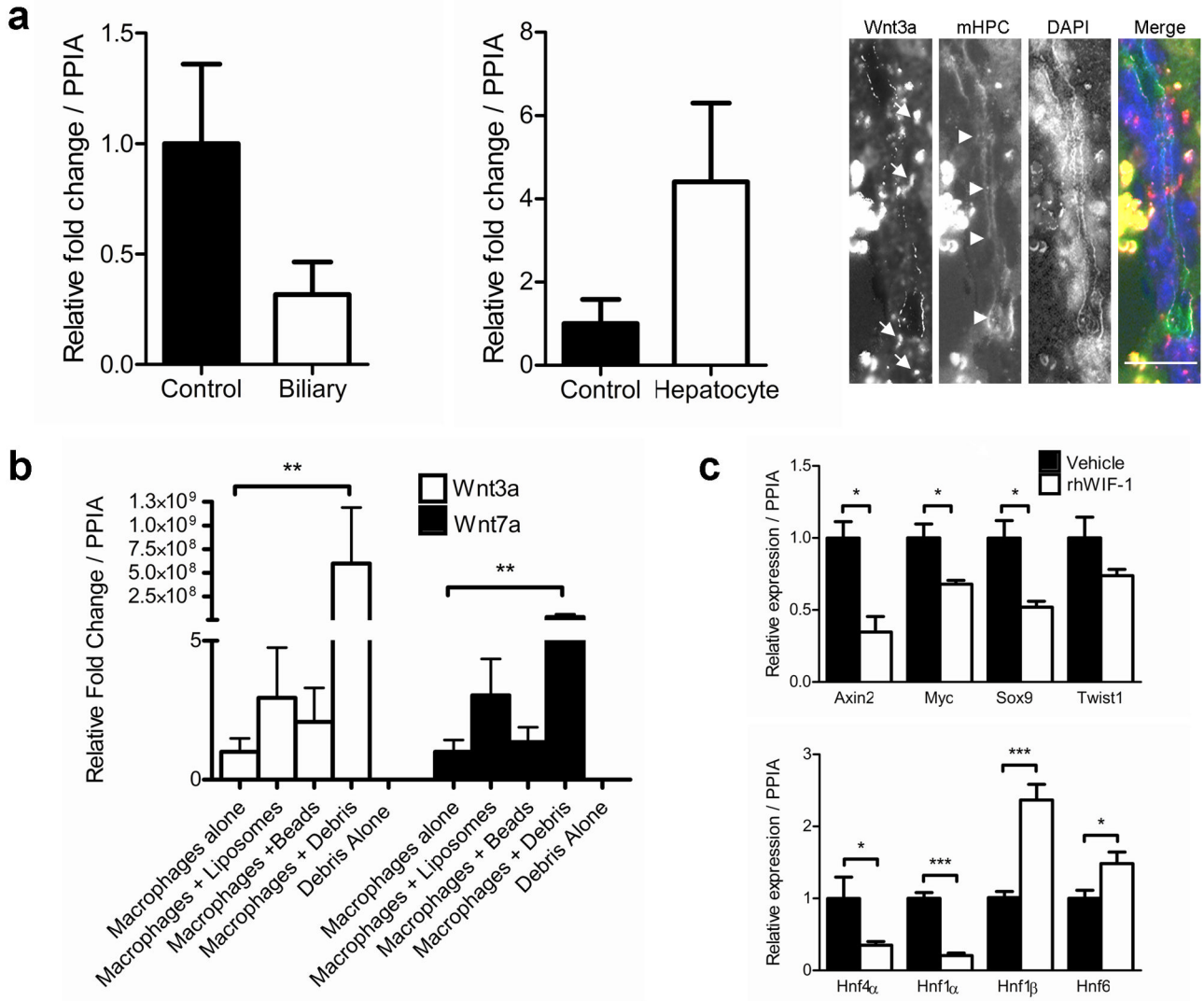


Figure 5. Macrophages are a source of canonical Wnt ligand in the regenerating adult liver
(a) Expression of the canonical ligand Wnt3a in F4/80 positive macrophages isolated from healthy animals versus animals undergoing biliary or hepatocyte regeneration. The Wnt3a protein (red) localised around mononuclear cells adjacent to mHPCs (green) during hepatocyte regeneration **(b)** Quantification of Wnt3a and Wnt7a expression by macrophages cultured with hepatocyte debris, latex beads or liposomes *in vitro*. **(c)** Gene expression analysis of Wnt pathway targets and liver enriched transcription factors in co-culture of post-phagocytic macrophages and mHPCs in the presence of rhWIF1 or vehicle alone. Data is expressed as means \pm S.E.M; * $P < 0.05$, ** $P < 0.01$, *** $P < 0.001$. CDE $n = 4$ DDC $n = 4$, Fed BMDMs $n = 6$, co-cultures $n = 12$. Scale bar = 25 μ m

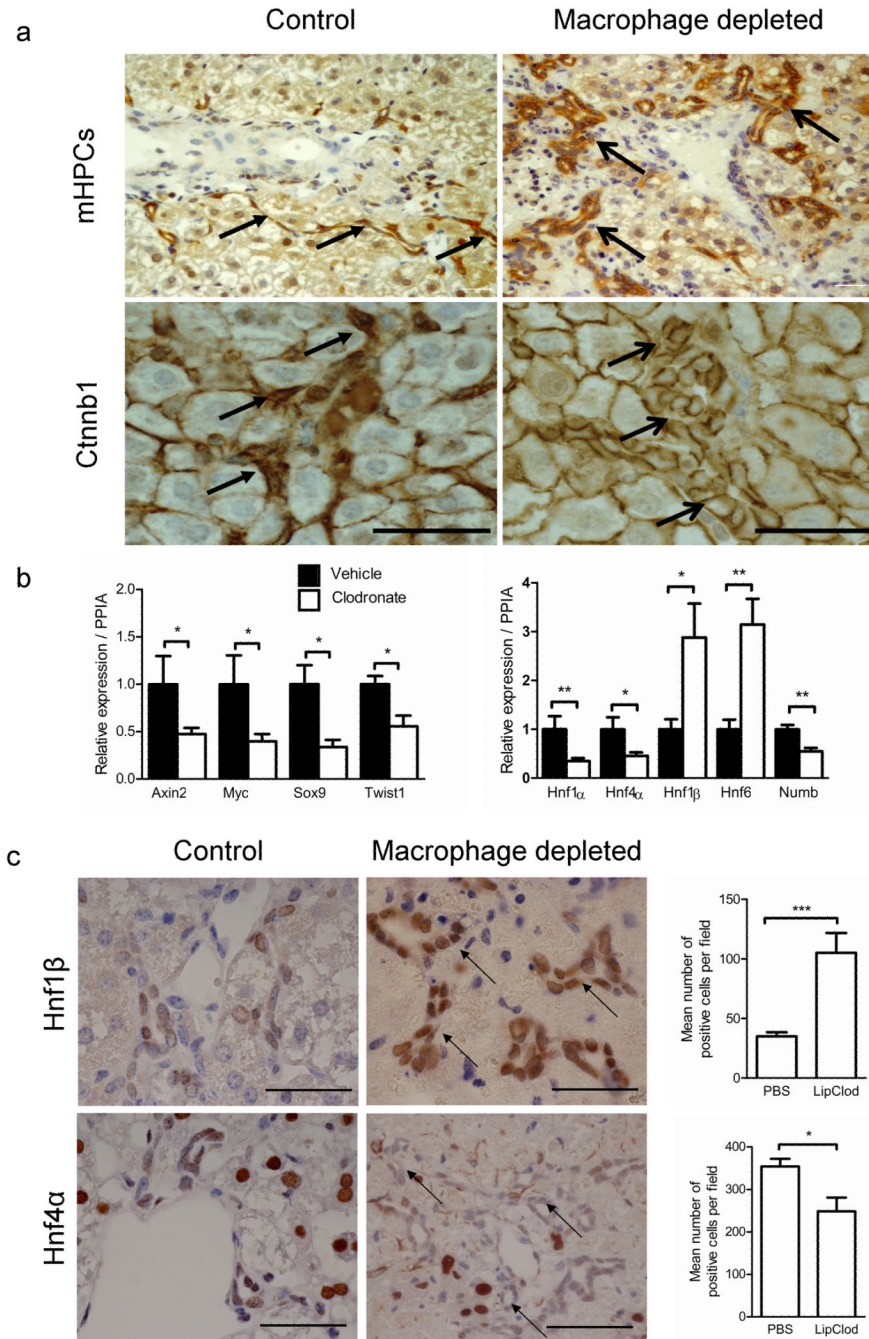


Figure 6. Ablation of Macrophages *in vivo* results in the re-specification of mHPCs
(a) Upper panels panCK positive mHPCs during hepatocyte regeneration in the presence or absence of macrophages; lower panels, localisation of Ctnnb1 in mHPCs during hepatocyte regeneration in the presence or absence of macrophages. **(b)** Transcript expression of Wnt pathway targets and liver enriched transcription factors in mHPCs isolated from animals depleted for macrophages compared to PBS controls **(c)** Photomicrographs of Hnf1 β (upper panels) and Hnf4 α (lower panels) in mHPCs of livers depleted of macrophages or controls. This positivity is quantified as absolute number of Hnf1 β or Hnf4 α positive cells (upper and lower histogram respectively) in control vs. macrophage depleted animals. Data is expressed

as means \pm S.E.M; * $P < 0.05$, ** $P < 0.01$, *** $P < 0.001$. liposomal clodronate and control $n = 10$. Scale bar = 100 μ m